



Formation Mechanisms of Divacancy-Oxygen Complex in Silicon

Masayuki Furuhashi^z and Kenji Taniguchi

Division of Electrical, Electronic and Information Engineering, Osaka University, Osaka 565-0871, Japan

Microscopic transition states and activation energies for formation reactions of divacancy-oxygen complex (V_2O) are investigated by first-principles calculations. The calculations reveal that divacancy-oxygen complex is formed from divacancy or the vacancy-oxygen pair by reactions as $V_2 + O_i \rightarrow V_2O$ and $VO + V \rightarrow V_2O$. The detailed analysis of calculation results clarified that the reaction of $VO + V \rightarrow V_2O$ occurs at room temperature, and the reaction of $V_2 + O_i \rightarrow V_2O$ occurs at 230–300°C. The dissociation mechanisms of divacancy-oxygen complex are also discussed.

© 2008 The Electrochemical Society. [DOI: 10.1149/1.2825173] All rights reserved.

Manuscript submitted October 10, 2007; revised manuscript received November 7, 2007. Available electronically January 2, 2008.

Many research achievements on atomic scale defects have been applied to the latest silicon processes for better device performances. Among them, silicon vacancy, divacancy, oxygen, and their complexes are the most popular defects to be investigated. However, the formation and dissociation mechanisms of multi-vacancy-oxygen complex (V_xO_y), including divacancy-oxygen complex (V_2O), have not been clarified yet. Recently, the clarification of the formation and dissociation mechanisms of V_2O has become important because the deep ionization levels of V_xO_y cause leakage current at a p-n junction formed in the Czochralski silicon wafer.^{1,2} V_2O is formed from either divacancy (V_2) or the vacancy-oxygen pair (VO) based on reactions as $V_2 + O_i \rightarrow V_2O$ or $VO + V \rightarrow V_2O$.^{3,a,4}

Calculation Details

We performed first-principles total-energy calculations with a generalized gradient approximation to derive the exchange-correlation energy.⁵ Vanderbilt ultrasoft pseudopotentials were used for silicon and oxygen atoms.⁶ The total energies of the defects in a neutral charge state were calculated using periodically repeated supercells containing 64 silicon sites with a lattice constant of 10.8 Å. The energy cutoff for the plane-wave expansion used was 300 eV. We performed Brillouin zone samplings with a $2 \times 2 \times 2$ Monkhorst-Pack k-point mesh for the supercell. Atomic positions were allowed to relax fully until all residual forces became smaller than 0.05 eV/Å. We then performed the synchronous transit method with a conjugate gradient technique to find microscopic transition states and activation energies.⁷ In transition-state searches, the atoms were relaxed until their residual forces had converged to <0.15 eV/Å.

We investigated an interstitial oxygen (O_i) diffusion in silicon. The calculated O_i diffusion barrier of 2.53 eV agrees well with the barrier energies measured by secondary-ion mass spectroscopy or infrared measurements, etc.,⁸ ensuring the accuracy of the calculation method.

Transition States and Activation Energies for Reactions

Figure 1 indicates a generation process of V_2O from smaller atomic defects. A primordial defect of V_2O is a single vacancy. Divacancy is formed by a combination of two vacancies: $V + V \rightarrow V_2$ and a silicon vacancy captured by O_i becomes a VO pair and $V + O_i \rightarrow VO$. V_2O is formed from either V_2 or VO via two separate reactions. In what follows, first we discuss the formation mechanisms of V_2 ($V + V \rightarrow V_2$) and VO ($V + O_i \rightarrow VO$). Then, we study the formation mechanisms of V_2O by two reactions: $V_2 + O_i \rightarrow V_2O$ and $VO + V \rightarrow V_2O$.

$V + V \rightarrow V_2$.— V_2 , the most common defect in crystalline silicon, is generated by ion implantation, electron irradiation, or γ irradiation. Watkins determined a vacancy diffusion barrier of 0.33 eV by electron paramagnetic resonance measurements.⁹ A low diffusion barrier indicates that even at room temperature, two silicon vacancies easily combine to form V_2 . Hwang and Goddard III investigated the binding mechanism of V_2 by using first-principles calculations and derived an energy barrier¹⁰ of 0.6 eV for the reaction of $V + V \rightarrow V_2$.

$V + O_i \rightarrow VO$.—In our previous work,¹¹ we calculated the total energies of several microscopic structures, including a vacancy and an interstitial oxygen to elucidate the formation mechanism of VO. The formation energy of an infinitely separated V from O_i is defined as zero energy. The binding energy of VO is defined by $E_b(V-O) = E(\text{Si}_{63}) + E(\text{Si}_{64}\text{O}) - E(\text{Si}_{63}\text{O}) - E(\text{Si}_{64})$, where $E(\text{Si}_{63})$ is the total energy of a 63-atom supercell including a vacancy, $E(\text{Si}_{64}\text{O})$ is that of a 65-atom supercell with an interstitial oxygen, and $E(\text{Si}_{63}\text{O})$ represents the total energy of a 64-atom supercell including VO. The calculated binding energy of V and O_i is 1.39 eV, which is close to the binding energy of 1.4 eV derived by Pesola et al.³ The interstitial oxygen occupies a bridging position between neighboring Si atoms to form a Si–O–Si bonding structure that captures a vacancy. In this paper, a Si–O–Si with an adjacent vacancy is referred to as a “Si–O–Si–V” configuration (see Fig. 2). The Si–O–Si–V configuration is an intermediate state involved in VO diffusion. The formation energy of the Si–O–Si–V configuration is –0.91 eV. The Si–O–Si–V configuration changes to VO by one of five paths based on its symmetry. The calculated formation energies of the five transition states are –0.17, –0.07, +0.77, +0.73, and +0.63 eV. From the formation energies of the five transition states, we found the most plausible reaction of $V + O_i \rightarrow VO$ with the activation energy of 0.74 eV, as shown in Fig. 2. In VO diffusion, a VO pair structurally changes to the Si–O–Si–V configuration and then the separated V recombines with O_i at a different position from the original VO pair by one of the other four reverse reactions. The migration energy of VO originates from a difference between the formation energy of the transi-

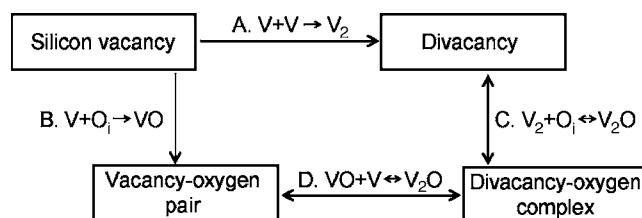


Figure 1. Correlation chart of divacancy-oxygen complex based on intrinsic defects consisting of vacancies and oxygen.

^z E-mail: furuhashi@si.eei.eng.osaka-u.ac.jp

^a The formation energies in a 32-atom supercell with MP-2³ Brillouin zone sampling give the binding energy 1.4 eV of VO.

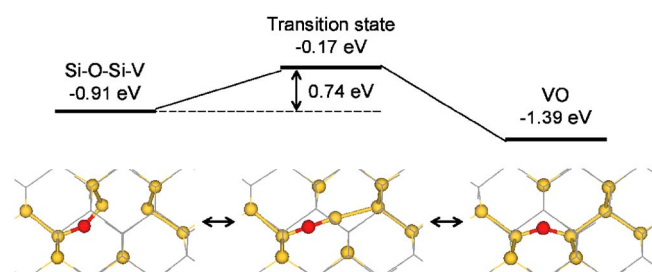


Figure 2. (Color online) Formation energy diagram and structural change in the reaction of $V + O_i \rightarrow VO$ shown along a $\langle 110 \rangle$ direction. Silicon and oxygen are represented as yellow and red balls, respectively. Gray lines indicate crystalline silicon lattice.

tion state and the VO pair (~ 2.0 eV), which agrees well with the barrier height measured by deep level transient spectroscopy (DLTS).¹²

$V_2 + O_i \leftrightarrow V_2O$.—First-principles calculations reveal that V_2O with C_{1h} symmetry is the most stable among various V_2O configurations. A derived Si–O–Si angle of 141° is close to the values reported by Pesola et al.¹³ (138°) and Ewels et al.¹³ (143°). In this paper, the formation energy of an infinitely separated O_i from V_2 is defined as zero energy. The binding energy between V_2 and O_i is calculated from $E_b(V_2-O_i) = E(\text{Si}_{62}) + E(\text{Si}_{64}O) - E(\text{Si}_{62}O) - E(\text{Si}_{64})$, where $E(\text{Si}_{62})$ is the total energy of a 62-atom supercell including V_2 , $E(\text{Si}_{64}O)$ is that of a 65-atom supercell including O_i , and $E(\text{Si}_{62}O)$ is that of a 63-atom supercell including V_2O . The calculated binding energy between V_2 and O_i is 1.68 eV. It is found that O_i around V_2 has several stable positions, including the most stable C_{1h} symmetric V_2O . The three metastable configurations are C_{3v} symmetric V_2O and the two Si–O–Si– V_2 configurations, where V_2 adjoins a Si–O–Si bond, as shown in Fig. 3. The symmetry of atomic structures suggests that two different types of Si–O–Si– V_2 configurations exist, as shown in Fig. 3a and b. The reaction of $V_2 + O_i \leftrightarrow V_2O$ occurs via the metastable configurations. The formation energies of the two Si–O–Si– V_2 configurations are (a) -0.30 eV and (b) -0.99 eV, and that of the C_{3v} symmetric V_2O is -1.14 eV. The calculated results above reveals that V_2 diffusing in silicon adjoins a Si–O–Si bond (O_i) to form Si–O–Si– V_2 configurations, and then the oxygen atom migrates to form C_{3v} symmetric V_2O . The formation energies of the transition states from the Si–O–Si– V_2 configurations to the C_{3v} symmetric V_2O via (a) and (b) type trans-

formations are $+0.62$ and $+0.48$ eV, respectively. The calculated formation energies denote that activation energies involved in the changes are (a) 0.92 and (b) 1.47 eV. Then, for the structural change from the C_{3v} symmetric V_2O into the C_{1h} symmetric V_2O , one of three Si–O bonds dissociates with the activation energy of 0.02 eV.

The calculated results above reveal that the reaction of $V_2 + O_i \rightarrow V_2O$ occurs with activation energies of 0.92 – 1.47 eV. The reverse reaction of $V_2O \rightarrow V_2 + O_i$ preferentially occurs with an activation energy of 2.16 eV because the reverse structural change to the Si–O–Si– V_2 of type (b) has lower barrier than that by type (a) transformation.

$VO + V \leftrightarrow V_2O$.—We defined the formation energy of an infinitely separated vacancy from VO as zero energy. The binding energy between VO and V is calculated from $E_b(\text{VO}-V) = E(\text{Si}_{63}) + E(\text{Si}_{63}O) - E(\text{Si}_{62}O) - E(\text{Si}_{64})$, where $E(\text{Si}_{63}O)$ is the total energy of a 64-atom supercell, including VO. The calculated binding energy of 1.91 eV is close to the energy of 1.72 eV reported by Taguchi et al.¹⁴ and 1.7 eV by Mikelsen et al.¹⁵ The C_{1h} symmetric V_2O has a V replaced with a Si atom at either a or b, as shown in Fig. 4 ($\text{VO} + V_a, \text{VO} + V_b$). Subscripts a and b indicate that V exists at the Si site of a or b, respectively. Note that, considering atomic symmetries, $\text{VO} + V_a$ and $\text{VO} + V_b$ each have two configurations per VO. V migrates from one of four different type sites (c–f) to form $\text{VO} + V_a$ or $\text{VO} + V_b$. The two types of Si sites, c and d, are two different positions per VO, and e and f each have four different sites per VO. Next, we investigated four cases in which V migrates from one of the four Si sites (c–f to a or b) to form the most stable V_2O .

Si site c: $\text{VO} + V_c$, where V exists at a Si site of c shown in Fig. 4, has the formation energy of -0.63 eV. The formation energy of the transition state in the structural change of $\text{VO} + V_c \rightarrow \text{VO} + V_a$ is -0.10 eV (see the top of Fig. 4). The activation energy involved in this structural change is 0.53 eV, and the activation energy of the reverse change is 1.81 eV.

Si site d: In the reaction where $\text{VO} + V_d$ changes into V_2O , the structural change of $\text{VO} + V_d \rightarrow \text{VO} + V_b$ occurs (see the bottom of Fig. 4). In this change, the oxygen atom migrates along with a reorientation of VO with the activation energy of 1.17 eV, which is higher than $\text{VO} + V_c \rightarrow \text{VO} + V_a$. The latter half of this change is essentially the same as a structural change of $\text{VO} + V_c \rightarrow \text{VO} + V_a$.

Si site e: $\text{VO} + V_e$, where V exists at a Si site of e, is unstable.

Si site f: $\text{VO} + V_f$ hardly changes into V_2O ($\text{VO} + V_b$) because the transition state involves an unstable configuration.

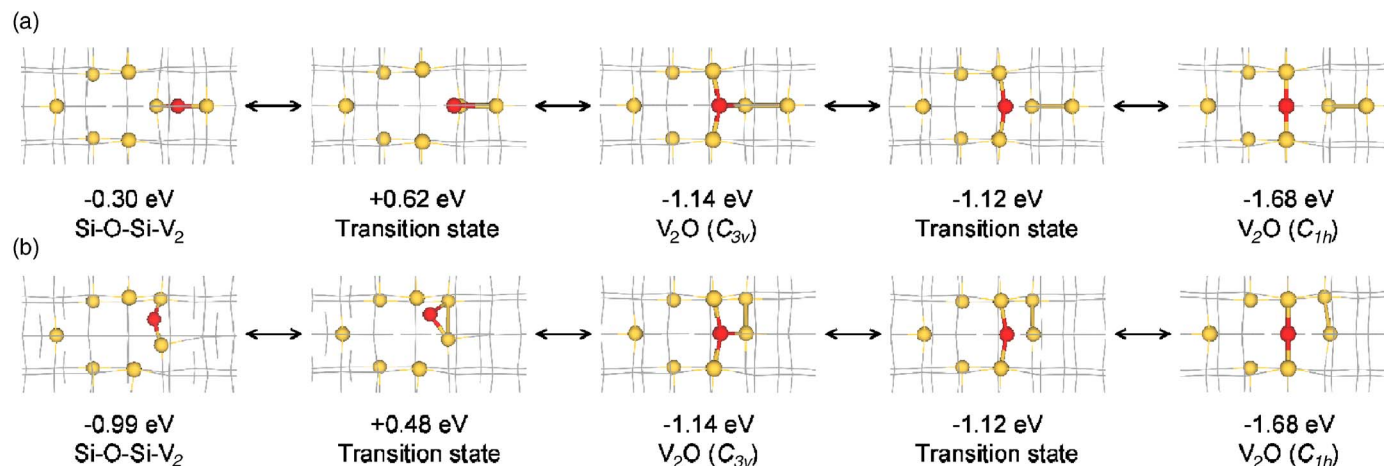


Figure 3. (Color online) Structural changes in the reaction of $V_2 + O_i \rightarrow V_2O$ shown along a $\langle 100 \rangle$ direction. Silicon and oxygen are represented as yellow and red balls, respectively. Gray lines indicate lattice image of crystalline silicon lattice.

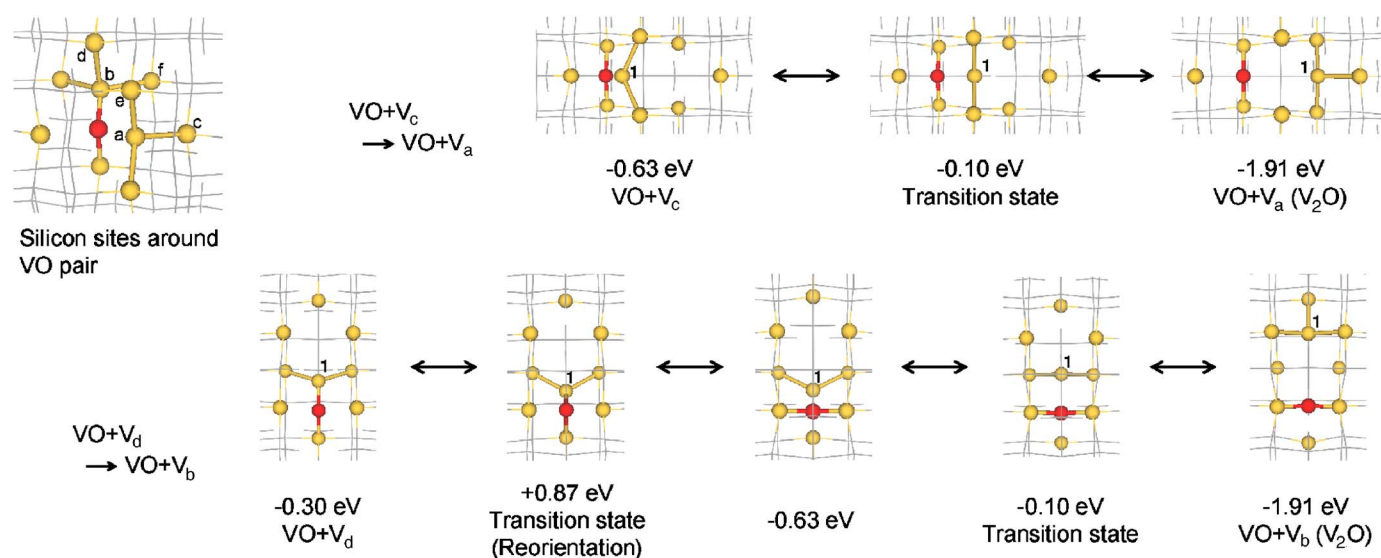


Figure 4. (Color online) Silicon sites around the vacancy-oxygen pair and structural changes in the reaction of $\text{VO} + \text{V} \rightarrow \text{V}_2\text{O}$, which is shown along a $\langle 100 \rangle$ direction. Silicon and oxygen are represented as yellow and red balls, respectively. Gray lines indicate crystalline silicon lattice.

The above discussions clarified that the formation reaction of $\text{VO} + \text{V} \rightarrow \text{V}_2\text{O}$ occurs with an activation energy of 0.53 eV while the dissociation reaction of $\text{V}_2\text{O} \rightarrow \text{VO} + \text{V}$ occurs with an activation energy of 1.81 eV.

Formation and Dissociation Mechanisms of V_2O

Finally, we discuss the formation and dissociation mechanisms of V_2O based on the above calculated results. In a previous work, Coutinho et al. studied the formation and dissociation mechanisms of V_2O .¹⁶ In their calculations, the reaction of $\text{V}_2 + \text{O}_i \rightarrow \text{V}_2\text{O}$ was investigated, and V_2O is generated over ~ 1.3 eV of the diffusion barrier for V_2 . In contrast, the reaction of $\text{VO} + \text{V} \rightarrow \text{V}_2\text{O}$ was not considered. Therefore, the experimental evidence in which the number of V_2O increases with neutron irradiation dose at room temperature^{4,17} was not determined only by their calculated result. V_2O is formed by the two reactions: either $\text{V}_2 + \text{O}_i \rightarrow \text{V}_2\text{O}$ or $\text{VO} + \text{V} \rightarrow \text{V}_2\text{O}$, with activation energies of 0.92–1.47 and 0.53 eV, respectively. The migration energies of V , V_2 , VO , and O_i are 0.33, 1.3, 2.0, and 2.53 eV, respectively.^{9,11} Considering the encounter processes of the original defects, the reaction of $\text{V}_2 + \text{O}_i \rightarrow \text{V}_2\text{O}$ is limited by the V_2 migration barrier of 1.3 eV. This assumption is encouraged by Mikelsen's experiment.¹⁸ The activation energy of 1.3–1.47 eV is approximately equivalent to 230–300°C as a temperature range.^b This range agrees with the 250–300°C reported by Lindström et al., the 220–300°C by Monakhov et al., and the 225–275°C by Markevich et al.¹⁹ The reaction of $\text{VO} + \text{V} \rightarrow \text{V}_2\text{O}$ can occur with an activation energy of 0.53 eV. However, VO , which is an original defect in the reaction of $\text{VO} + \text{V} \rightarrow \text{V}_2\text{O}$, generates above an activation energy of 0.74 eV. Nevertheless, the reaction of $\text{VO} + \text{V} \rightarrow \text{V}_2\text{O}$ occurs at room temperature.

As mentioned above, V_2O is formed with two different energies due to the two reactions involved, as shown in Fig. 1. The experimental results reported by Lee and Corbett,²⁰ which explain that the number of V_2O stays constant below 150°C and increases at 200–300°C, are also consistent with the reaction of $\text{VO} + \text{V} \rightarrow \text{V}_2\text{O}$ at room temperature and the reaction of $\text{V}_2 + \text{O}_i \rightarrow \text{V}_2\text{O}$ at 230–300°C.

The two reverse reactions, $\text{V}_2\text{O} \rightarrow \text{V}_2 + \text{O}_i$ or $\text{V}_2\text{O} \rightarrow \text{VO} + \text{V}$, are involved in the dissociation of V_2O . In general, the activation energy of the dissociation reaction is defined by the sum of the binding energy and the smaller migration energy of the separated defects. On the basis of the above definition, the reverse reaction of $\text{V}_2\text{O} \rightarrow \text{V}_2 + \text{O}_i$ occurs with an activation energy of 2.98 eV, which is the sum of the binding energy of 1.68 eV and the migration energy of 1.3 eV for V_2 . The reverse reaction of $\text{V}_2\text{O} \rightarrow \text{VO} + \text{V}$ occurs with an activation energy of 2.24 eV, which is the sum of the binding energy of 1.91 eV and the migration energy of 0.33 eV for V . The activation energies of the two reverse reactions suggest that the reaction of $\text{V}_2\text{O} \rightarrow \text{VO} + \text{V}$ occurs at a higher possibility than the reaction of $\text{V}_2\text{O} \rightarrow \text{V}_2 + \text{O}_i$. The activation energy of ~ 2.2 eV is relatively close to 2.02 ± 0.12 eV reported by Mikelsen et al.¹⁵ According to the experimental results of Lee and Corbett, V_2O is stable at 300–350°C and rapidly decreases at $> 350^\circ\text{C}$.²⁰ It is highly possible that at $\sim 350^\circ\text{C}$ V_2O captures V or O_i to change into V_3O or V_2O_2 because the number of V_3O and V_2O_2 increases with decreasing V_2O . We note the relation between the reduction of V_2O (at $\sim 350^\circ\text{C}$) and the dissociation reaction of $\text{V}_2\text{O} \rightarrow \text{VO} + \text{V}$.

Conclusion

We investigated microscopic transition states and activation energies for the formation reactions of V_2O based on intrinsic defects, which are vacancies and oxygen, by using first-principles total-energy calculations. The two investigated reactions of $\text{V}_2 + \text{O}_i \rightarrow \text{V}_2\text{O}$ and $\text{VO} + \text{V} \rightarrow \text{V}_2\text{O}$ reveals that V_2O is formed at two different temperature ranges due to the different activation energies of reactions ($\text{VO} + \text{V} \rightarrow \text{V}_2\text{O}$, 0.53 eV, and $\text{V}_2 + \text{O}_i \rightarrow \text{V}_2\text{O}$, 1.3–1.47 eV). In addition, we clarified that V_2O dissociates by the reaction of $\text{V}_2\text{O} \rightarrow \text{VO} + \text{V}$.

Acknowledgment

M.F. was supported by a Grant-in-Aid for Japan Society for the promotion of Science (JSPS) Fellows (188922). This research was partially supported by a grant for the Global COE Program, "Center for Electronic Devices Innovation," from the Ministry of Education, Culture, Sports, Science and Technology of Japan.

Osaka University assisted in meeting the publication costs of this article.

References

1. T. Umeda, Y. Mochizuki, K. Okonogi, and K. Hamada, *Physica B*, **308–310**, 1169

^b A transition rate of P is defined by $P = \nu \exp(-E_a/kT)$, where ν is the frequency of lattice vibration and E_a is an activation energy of a reaction. When $P = 1 \text{ s}^{-1}$ and $\nu = 10^{13} \text{ s}^{-1}$, an activation temperature T is defined by $T = E_a/(k \ln 10^{13})$.

- (2001).
2. K. Gill, G. Hall, and B. MacEvoy, *J. Appl. Phys.*, **82**, 126 (1997).
 3. M. Pesola, J. von Boehm, T. Mattila, and R. M. Nieminen, *Phys. Rev. B*, **60**, 11449 (1999).
 4. G. Davies, E. C. Lightowlers, R. C. Newman, and A. S. Oates, *Semicond. Sci. Technol.*, **2**, 524 (1987).
 5. J. P. Perdew, K. Burke, and M. Ernzerhof, *Phys. Rev. Lett.*, **77**, 3865 (1996).
 6. D. Vanderbilt, *Phys. Rev. B*, **41**, 7892 (1990).
 7. T. A. Halgren and W. N. Lipscomb, *Chem. Phys. Lett.*, **49**, 225 (1977).
 8. J. C. Mikkelsen, Jr., *Appl. Phys. Lett.*, **40**, 336 (1982); J. C. Mikkelsen, Jr., *Mater. Res. Soc. Symp. Proc.*, **59**, 19 (1986).
 9. G. D. Watkins and J. W. Corbett, *Phys. Rev.*, **138**, A543 (1965).
 10. G. S. Hwang and W. A. Goddard III, *Phys. Rev. B*, **65**, 233205 (2002).
 11. M. Furuhashi and K. Taniguchi, *Appl. Phys. Lett.*, **86**, 142107 (2005).
 12. O. O. Awadelkarim, H. Weman, B. G. Svensson, and J. L. Lindström, *J. Appl. Phys.*, **60**, 1974 (1986).
 13. C. P. Ewels, R. Jones, and S. Öberg, *Mater. Sci. Forum*, **196–201**, 1297 (1995).
 14. A. Taguchi, H. Kageshima, and K. Wada, *J. Appl. Phys.*, **97**, 053514 (2005).
 15. M. Mikkelsen, J. H. Bleka, J. S. Christensen, E. V. Monakhov, and B. G. Svensson, *Phys. Rev. B*, **75**, 155202 (2007).
 16. J. Coutinho, R. Jones, S. Öberg, and P. R. Briddon, *Physica B*, **340–342**, 523 (2003).
 17. B. C. MacEvoy, G. Hall, and K. Gill, *Nucl. Instrum. Methods Phys. Res. A*, **374**, 12 (1996).
 18. M. Mikkelsen, E. V. Monakhov, G. Alfieri, B. S. Avset, and B. G. Svensson, *Phys. Rev. B*, **72**, 195207 (2005).
 19. J. L. Lindström, L. I. Murin, V. P. Markevich, T. Hallberg, and B. G. Svensson, *Physica B*, **273–274**, 291 (1999); E. V. Monakhov, B. S. Aveset, A. Hallén, and B. G. Svensson, *Phys. Rev. B*, **65**, 233207 (2002); V. P. Markevich, A. R. Peaker, S. B. Lastovskii, L. I. Murin, and J. Lindström, *J. Phys.: Condens. Matter*, **15**, S2779 (2003).
 20. Y. H. Lee and J. W. Corbett, *Phys. Rev. B*, **13**, 2653 (1976).